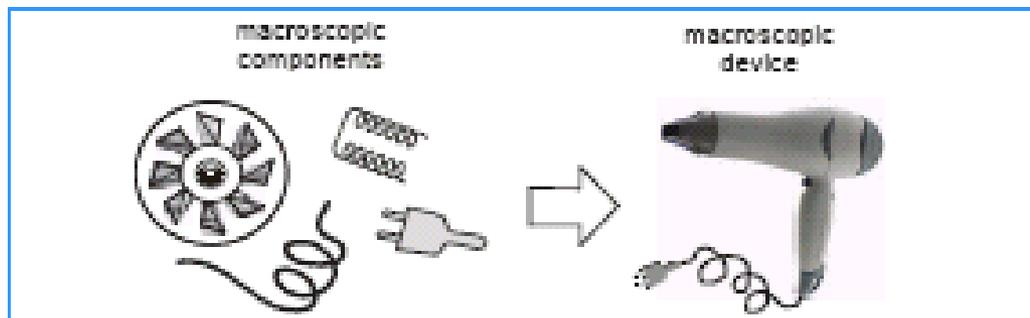


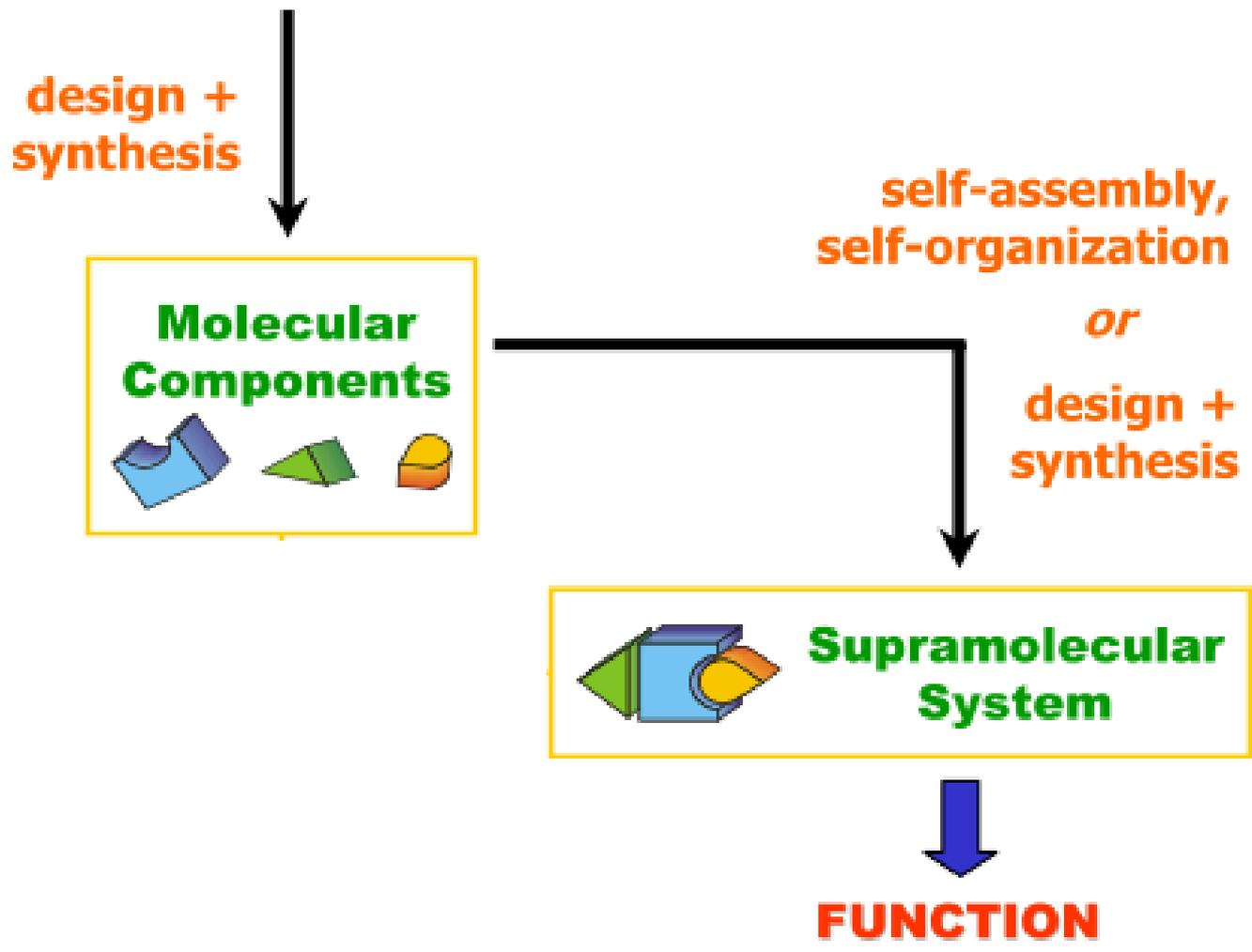
Dispositivi e Macchine Molecolari

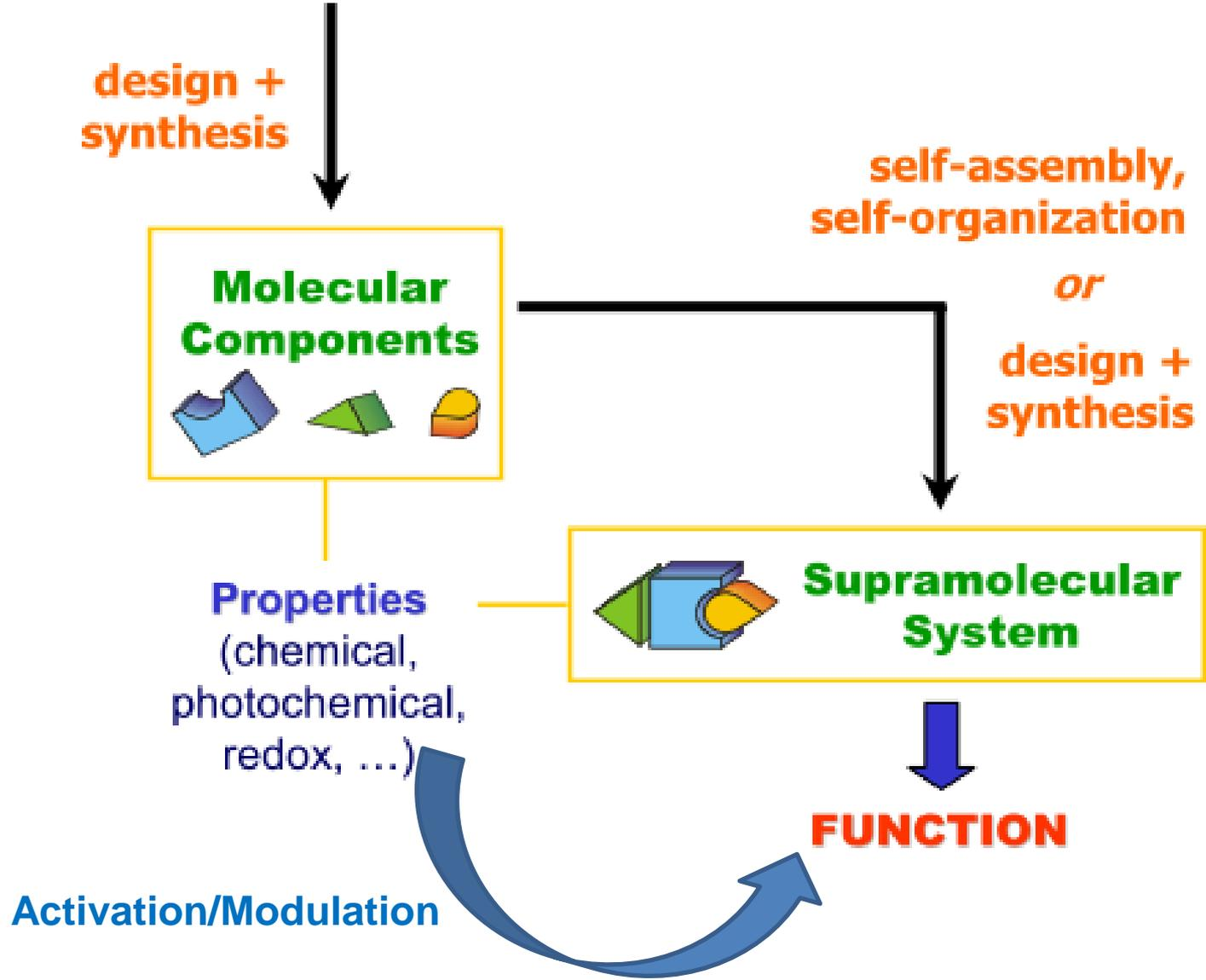
Macroscopic device



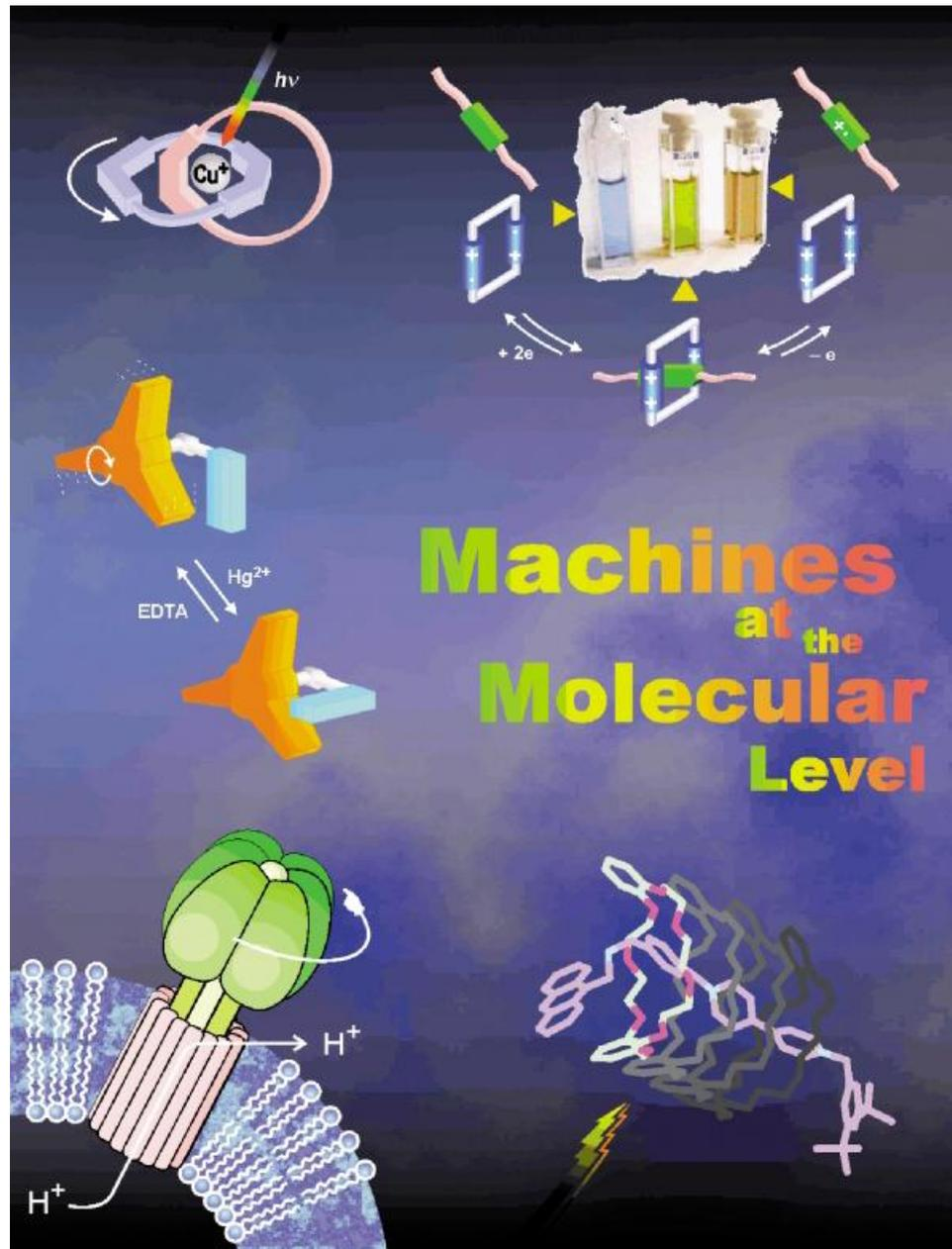
Molecular-level device







- tipo di energia (chimica, fotoni, elettroni)
- monitoraggio (tecniche fotofisiche, elettrochimiche)
- processo ciclico
- tempo (picosecondi-minuti)
- funzione



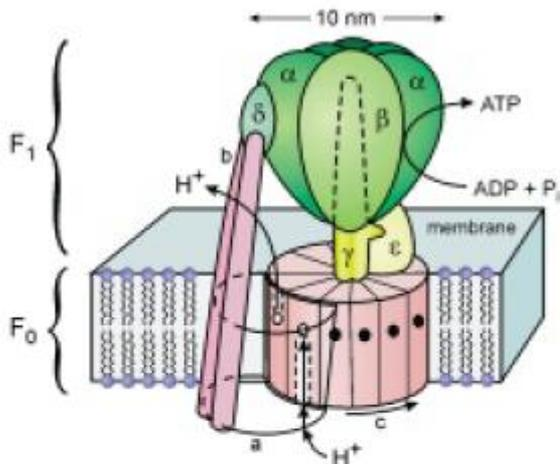


Figure 1. The structure of F_0F_1 ATP synthase.^[16] The catalytic region is composed of the subunits α - ϵ . The proton channels lie at the interface between the subunits a and c (dashed lines indicate the putative inlet and outlet channels). Proton flow through the channels develops torque between the a and c subunits. This torque is transmitted to F_1 via the γ shaft and the ϵ subunit, where it is used to release ATP sequentially from the catalytic sites in F_1 . The c subunit consists of 9–12 twin α -helices arranged in a central membrane-spanning array. The a subunit consists of 5–7 membrane-spanning α -helices and is connected to F_1 by the b and δ subunits. Reprinted by permission from ref. [16] (Copyright[©] Macmillan Magazines Ltd 1998).

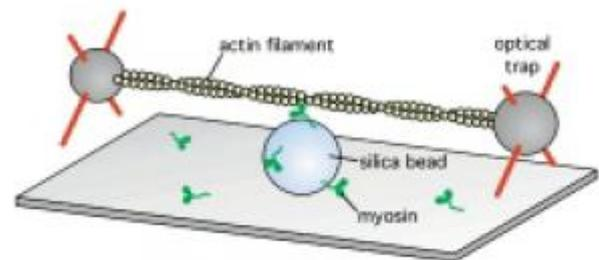
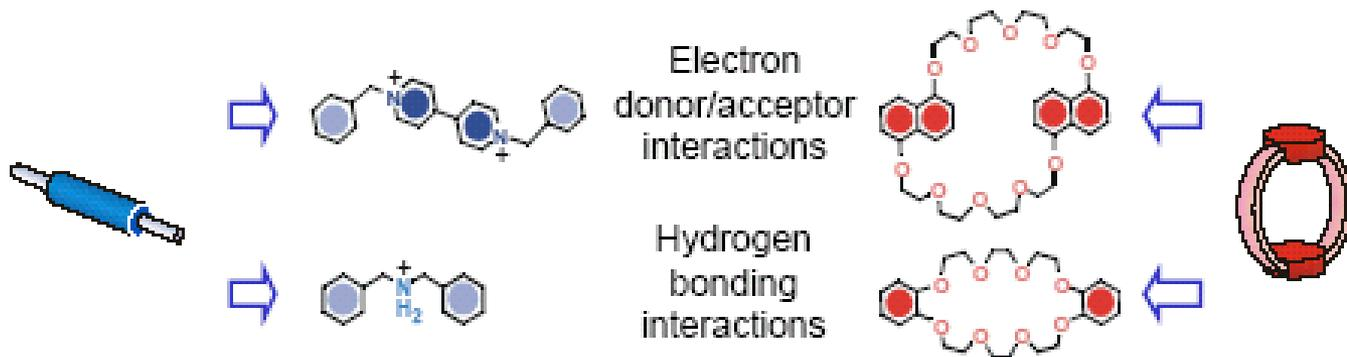
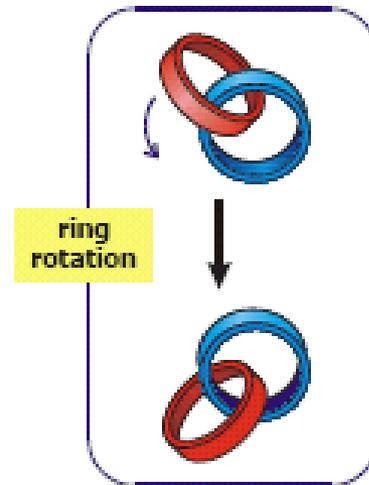
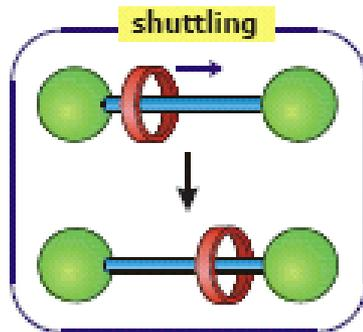
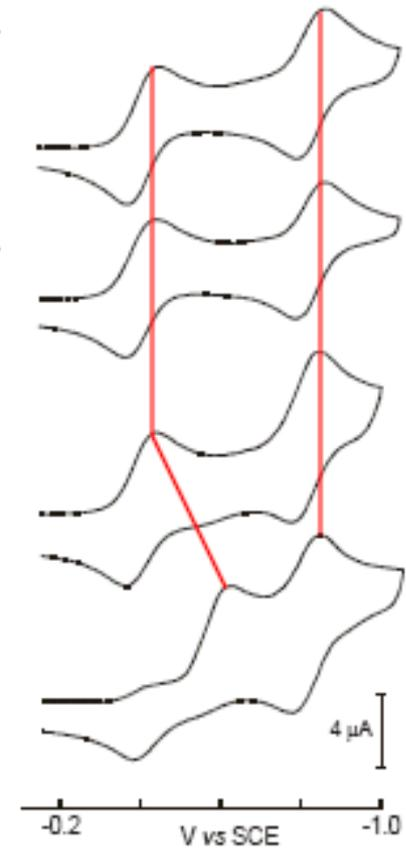
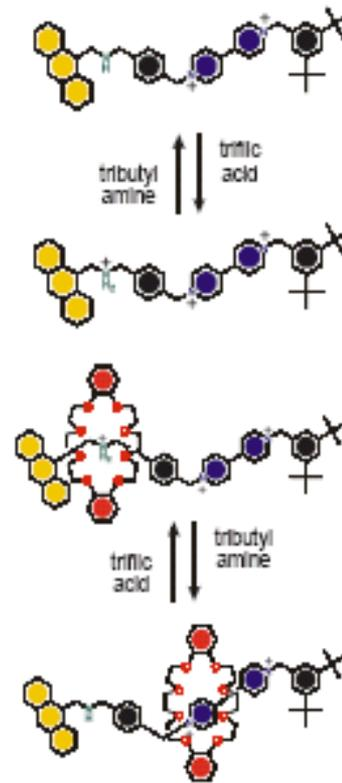
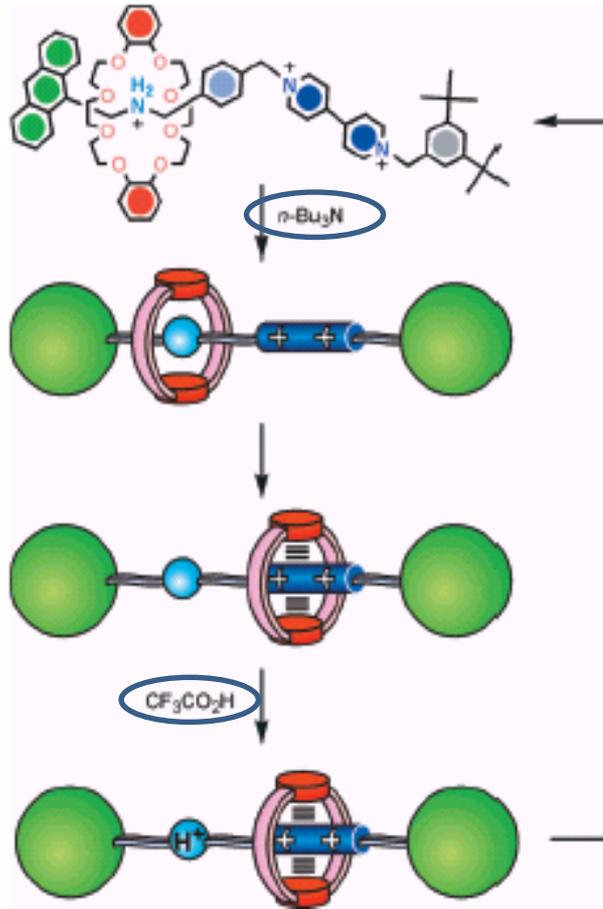
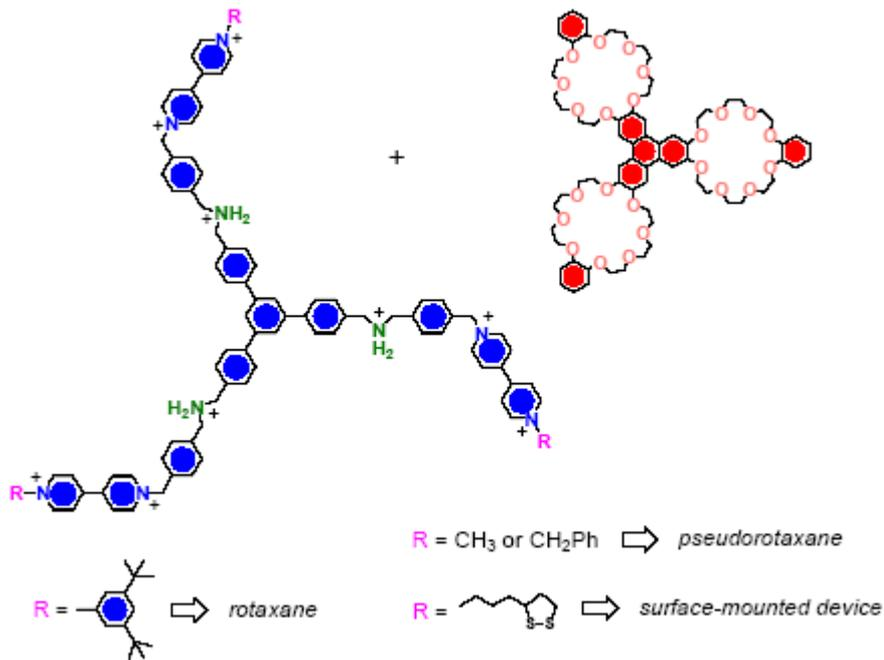


Figure 2. Experimental geometry used^[19] to observe single myosin molecules binding and pulling an actin filament. The filament was attached at either end to a trapped bead. These beads were used to stretch the filament taut and move it near surface-bound silica beads that were decorated sparsely with myosin molecules. Adapted with permission from ref. [19] (Copyright[©] Macmillan Magazines Ltd 1994).

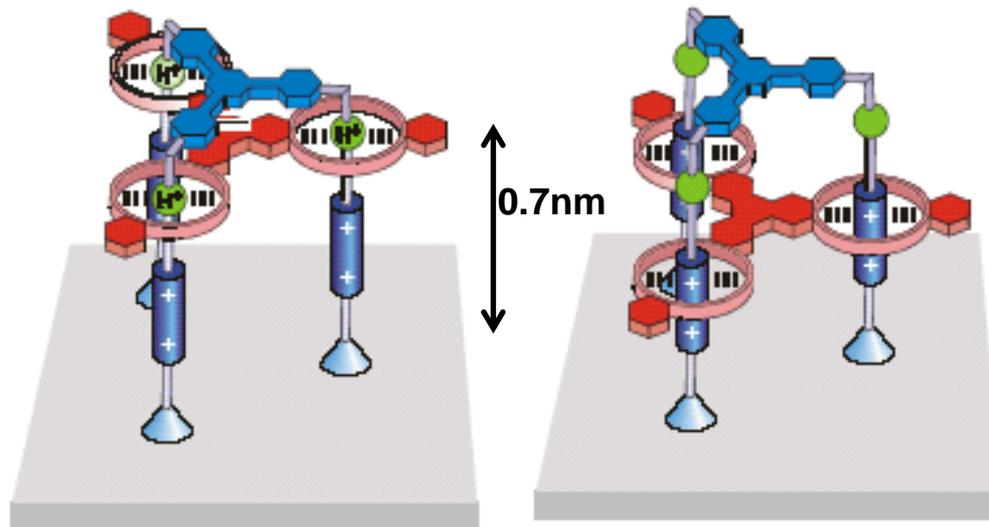
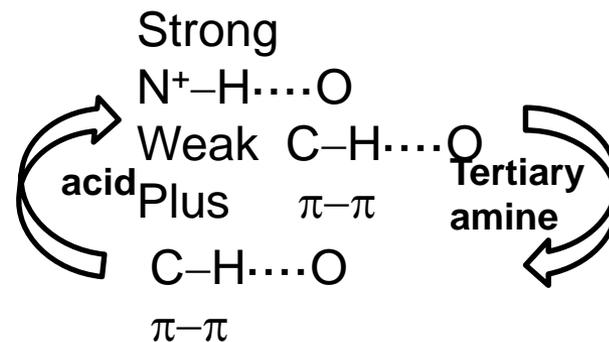


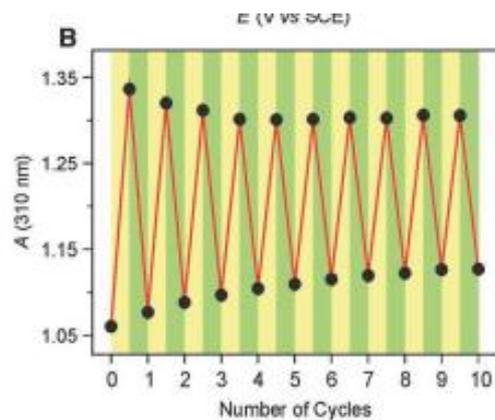
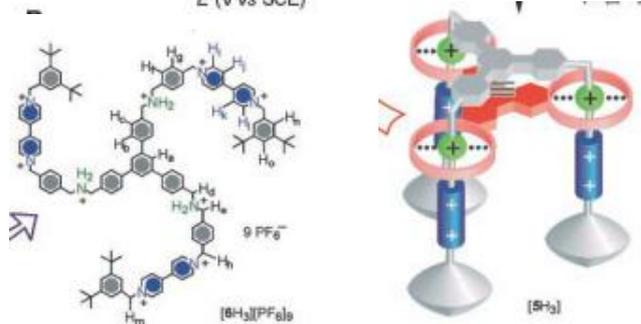
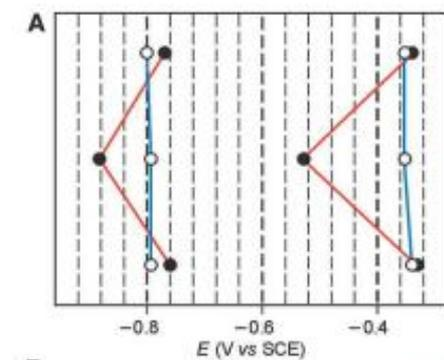
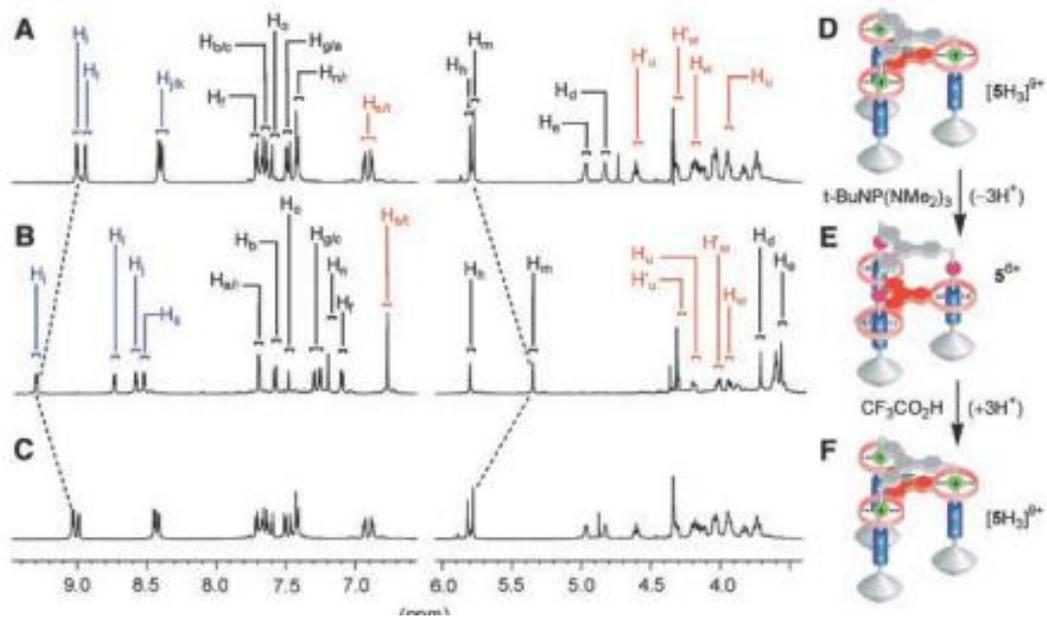
Input chimico

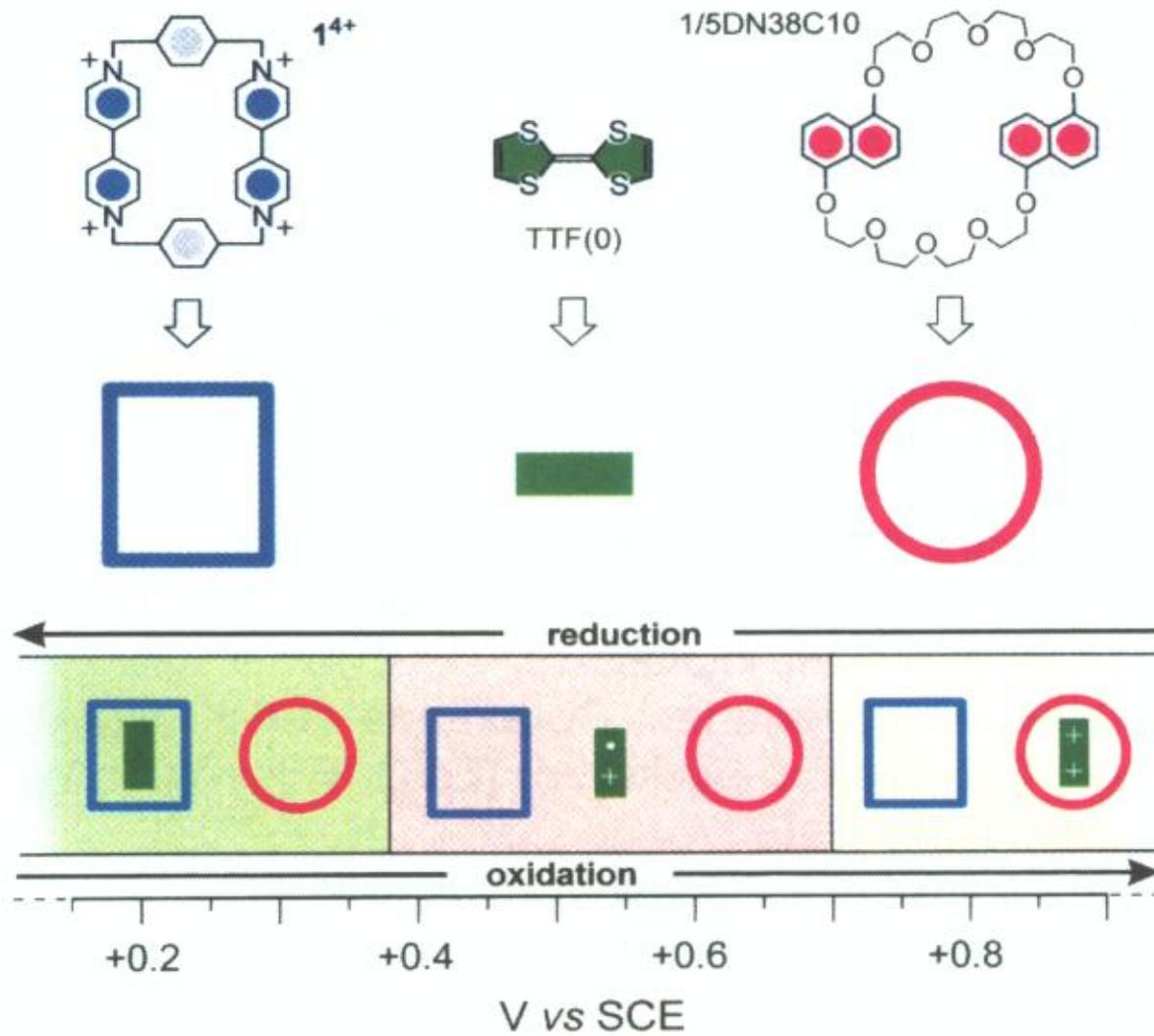




Ascensore molecolare

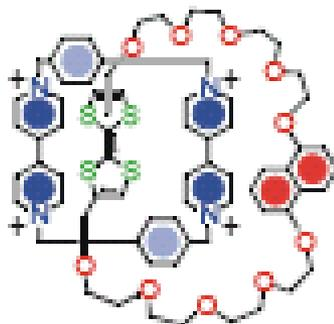




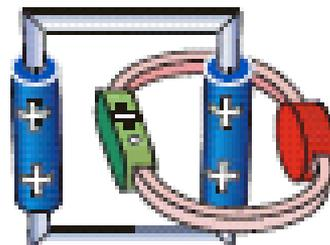


Input elettrochimico

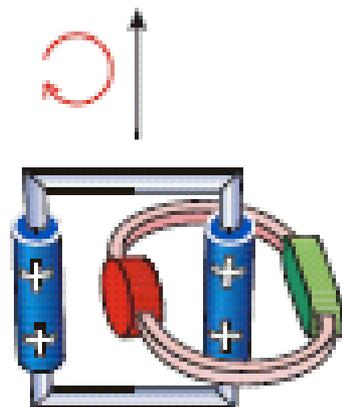
Tetratiofulvalene (0)



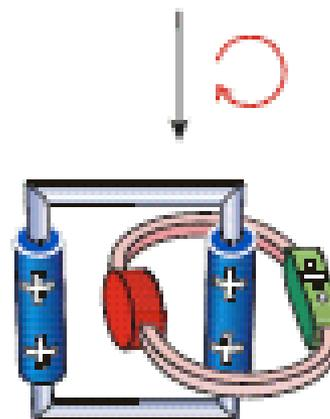
Tetratiofulvalene (+)



$-e^-$
ossidazione



Tetratiofulvalene (0)



Tetratiofulvalene (+)

$+e^-$
riduzione

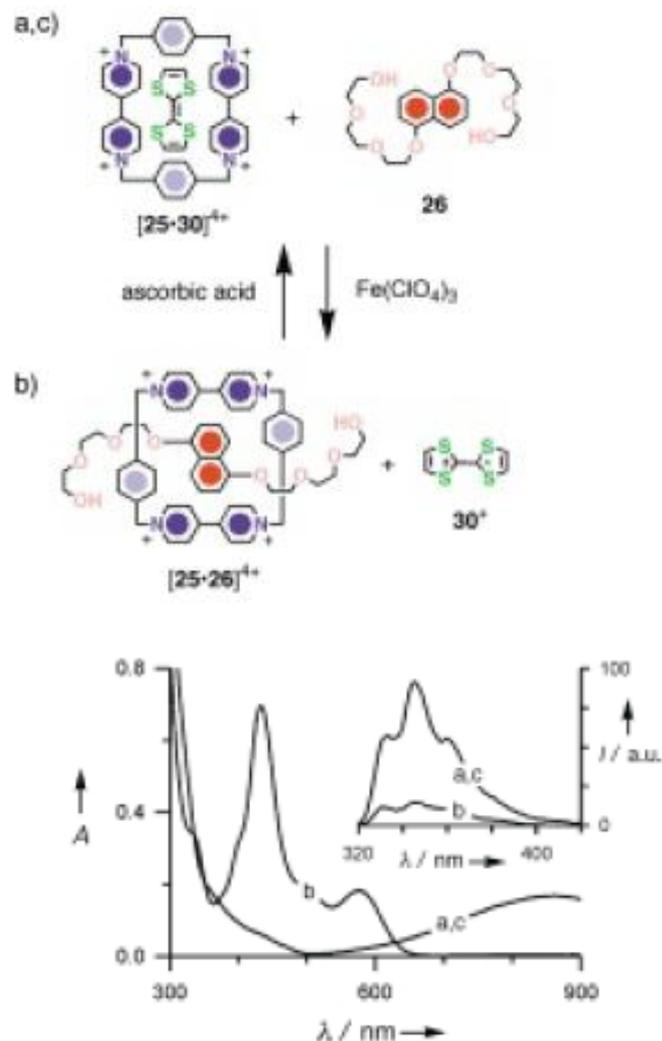
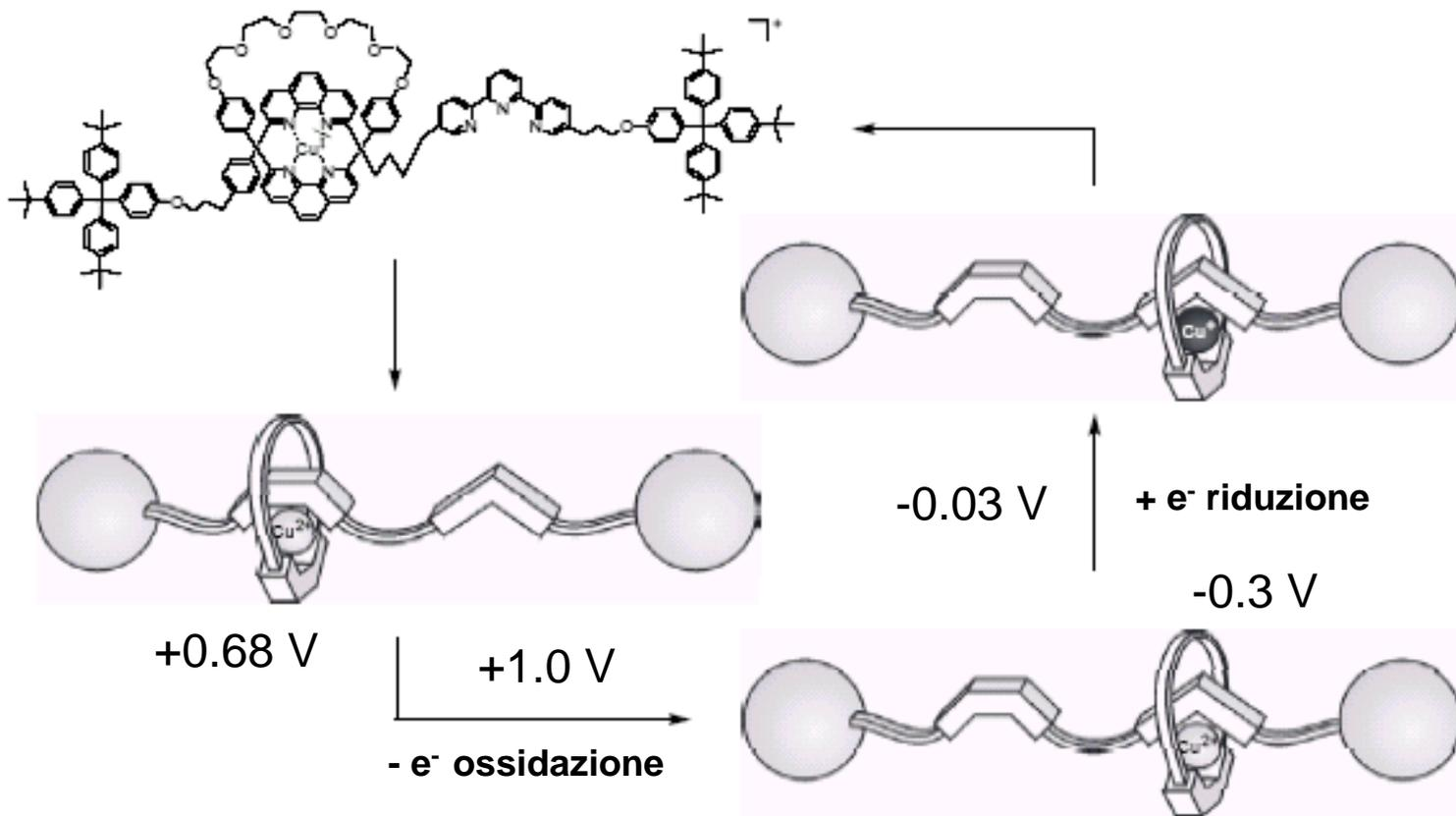
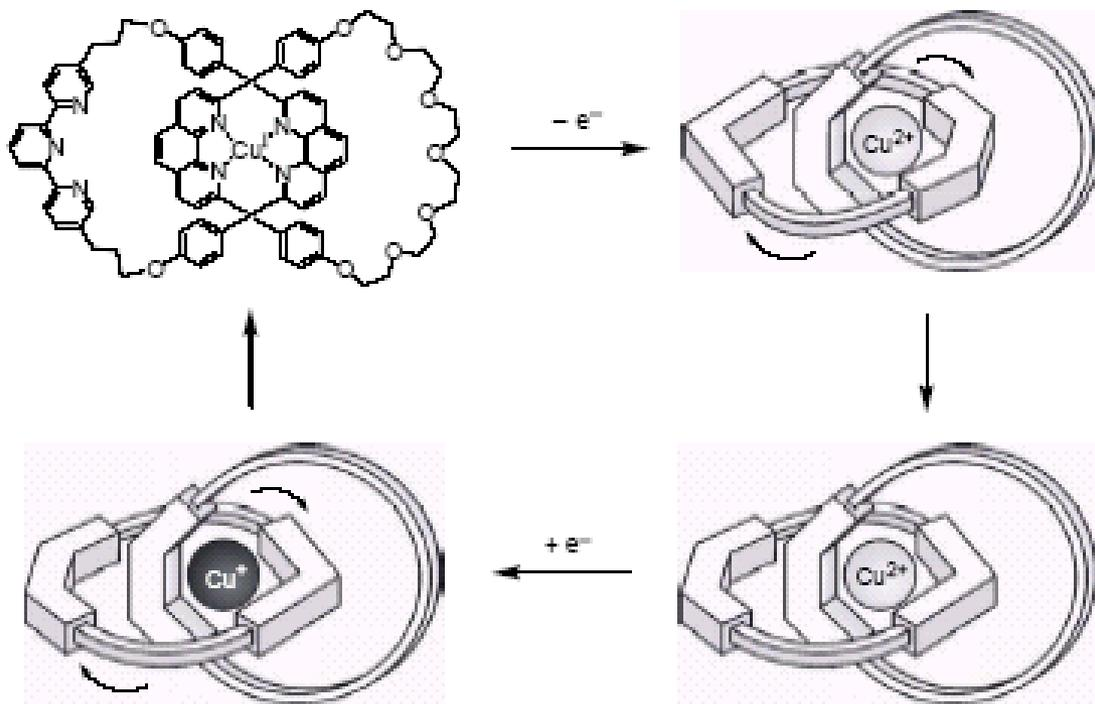


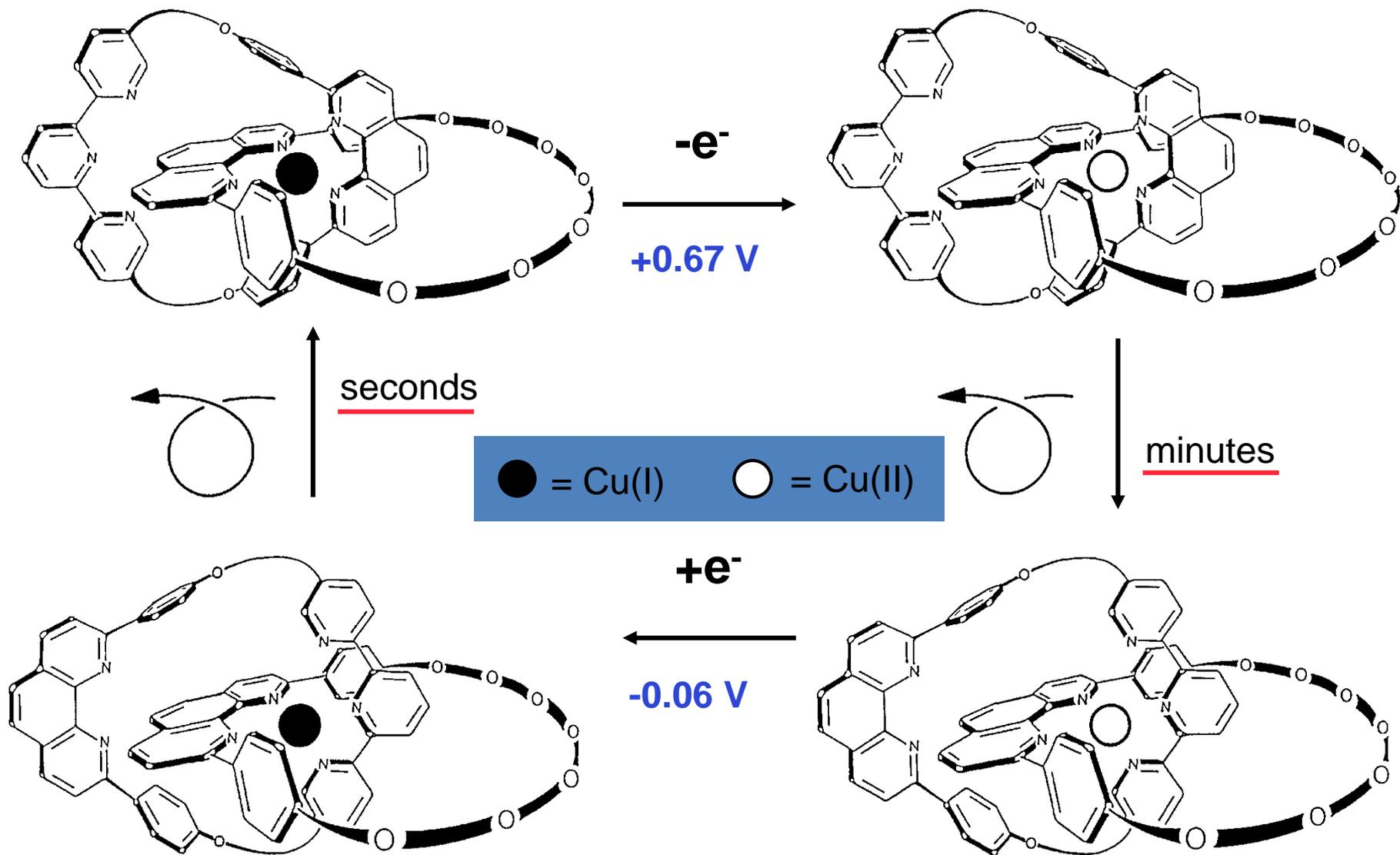
Figure 4. Top: the chemically induced interchange of guests **26** and **30** into the cavity of cyclophane 25^{4+} .^[93] Bottom: absorption and (inset) fluorescence ($\lambda_{exc} = 295 \text{ nm}$) spectra of a) a $5 \times 10^{-5} \text{ M}$ aqueous solution (298 K) of $[25 \cdot 30]^{4+}$ and **26**; b) the same solution after addition of one equivalent of $\text{Fe}(\text{ClO}_4)_3$; c) solution b) after addition of one equivalent of ascorbic acid.

Input elettrochimico

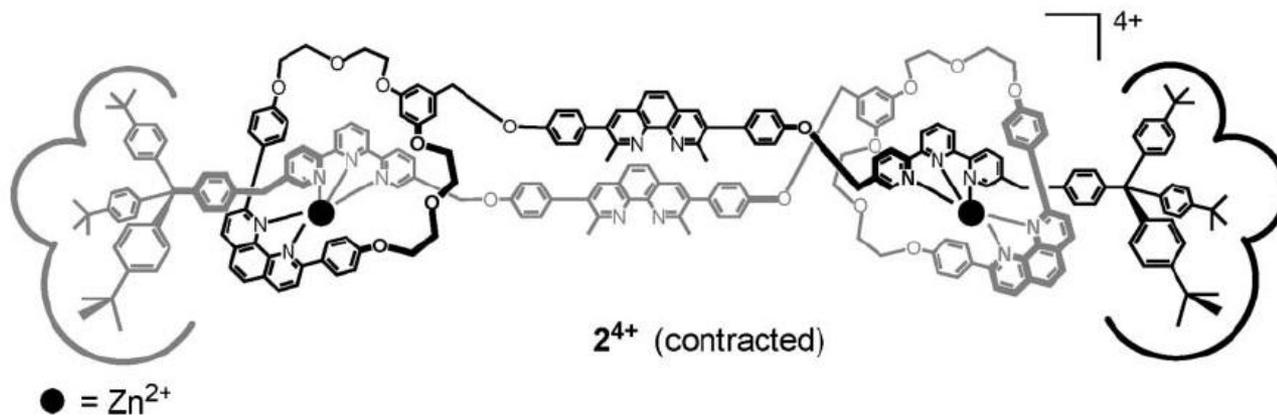
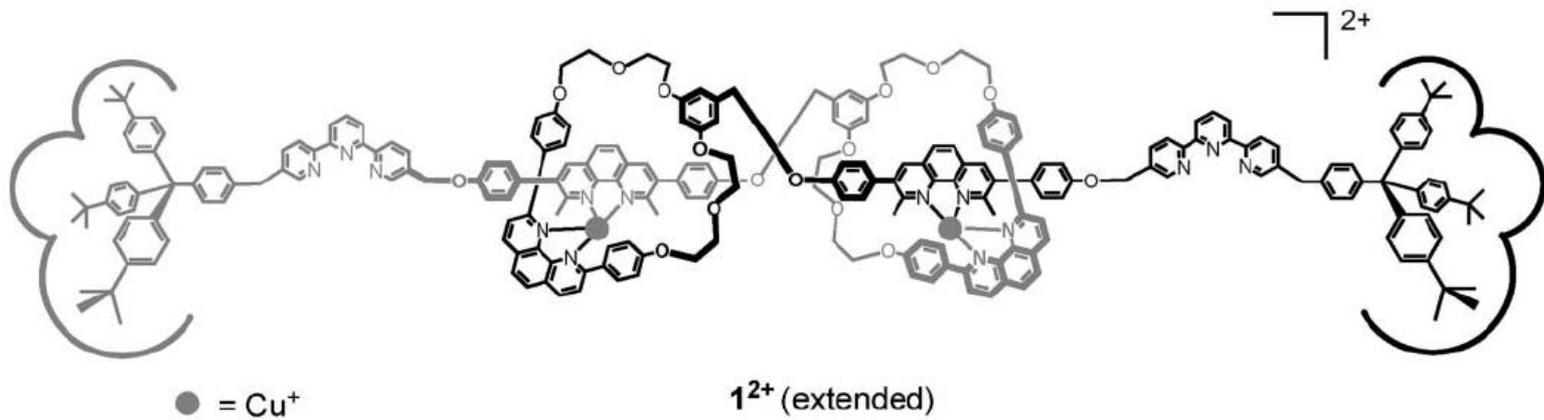
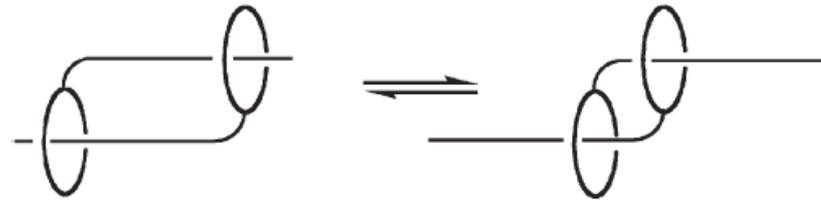


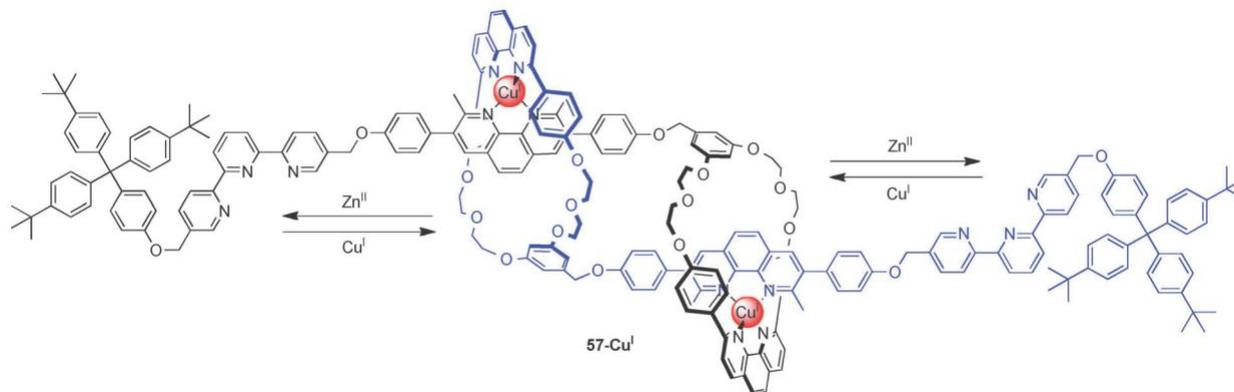
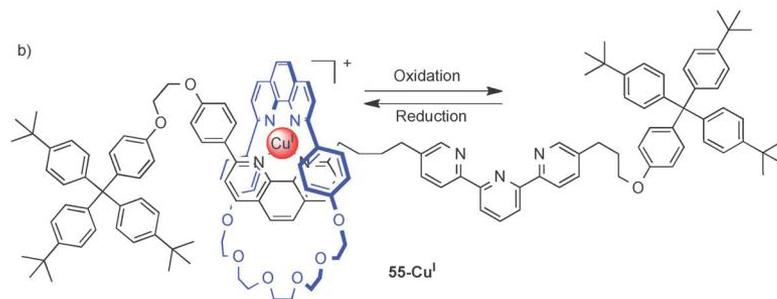
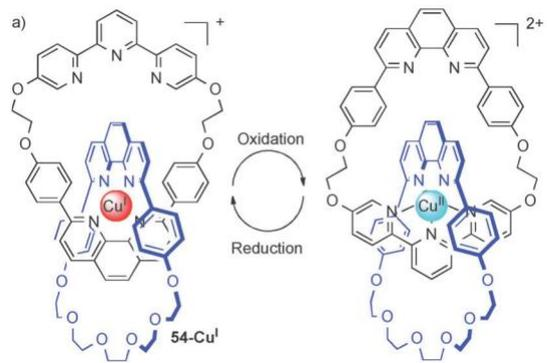
Input elettrochimico





Input chimico





Input fotochimico

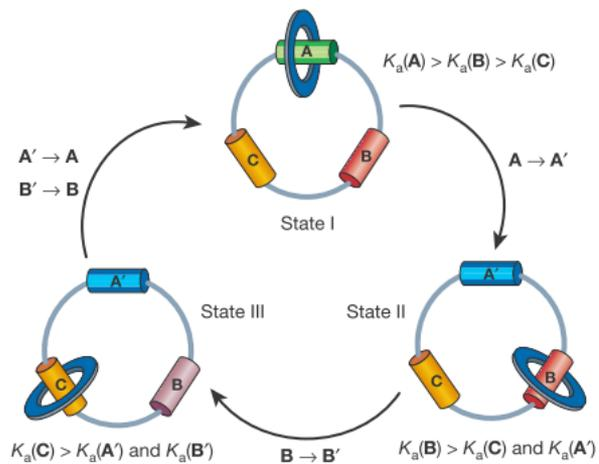
.....

Unidirectional rotation in a mechanically interlocked molecular rotor

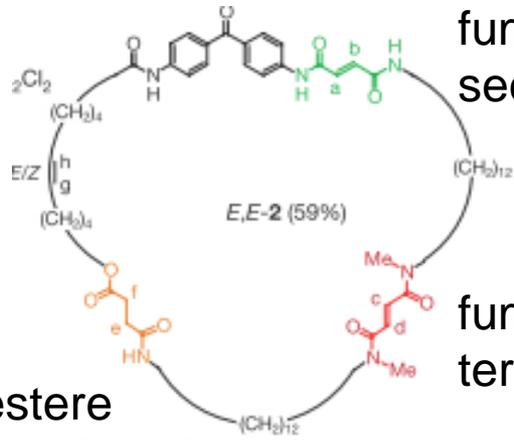
David A. Leigh^{*}, Jenny K. Y. Wong^{*}, François Dehez[†]
& Francesco Zerbetto[†]

^{*} School of Chemistry, University of Edinburgh, The King's Buildings, West Mains Road, Edinburgh EH9 3JJ, UK

[†] Dipartimento di Chimica 'G. Ciamician', Università degli Studi di Bologna, via F. Selmi 2, 40126 Bologna, Italy



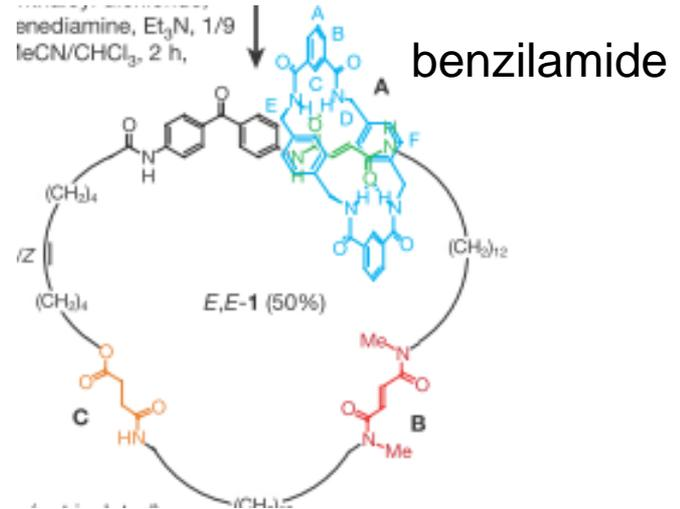
benzofenone



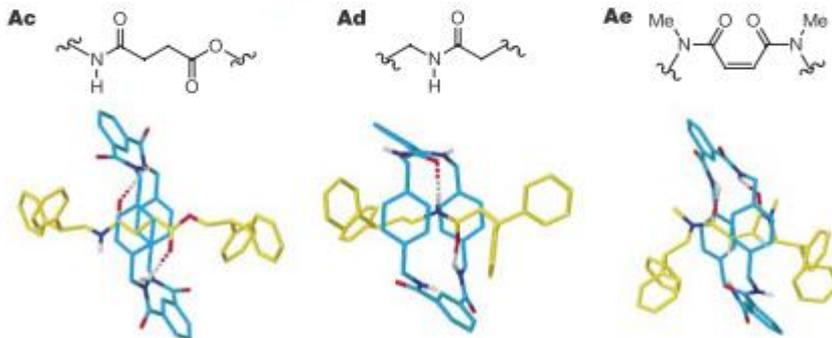
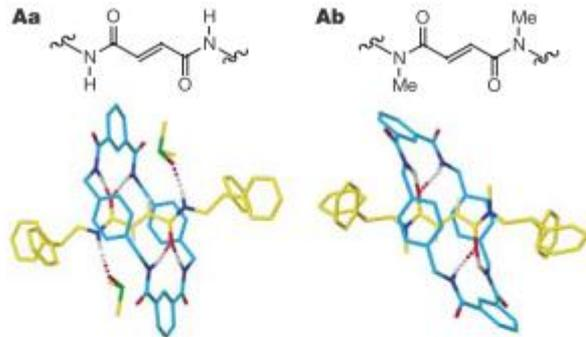
fumaramide
secondaria *E*

estere
succinamidico

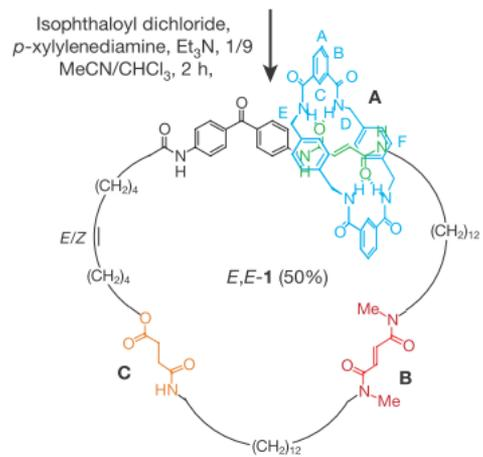
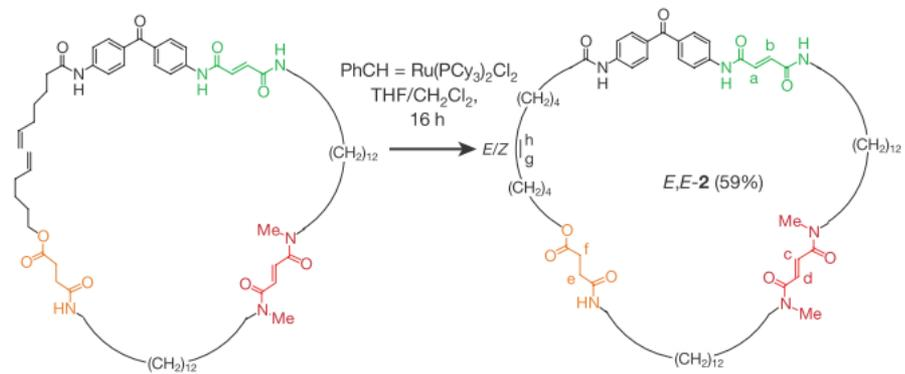
fumaramide
terziaria *E*

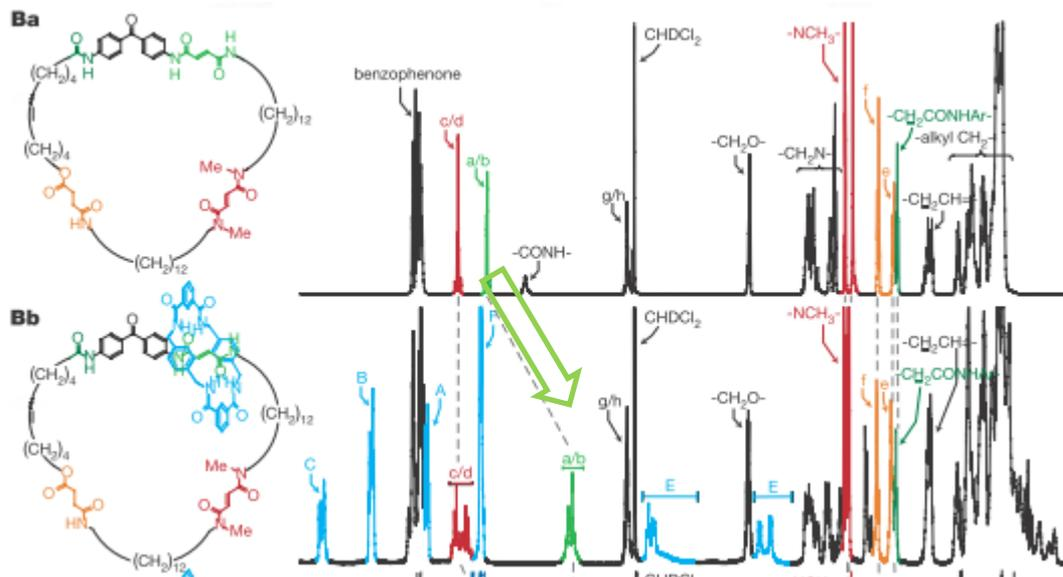
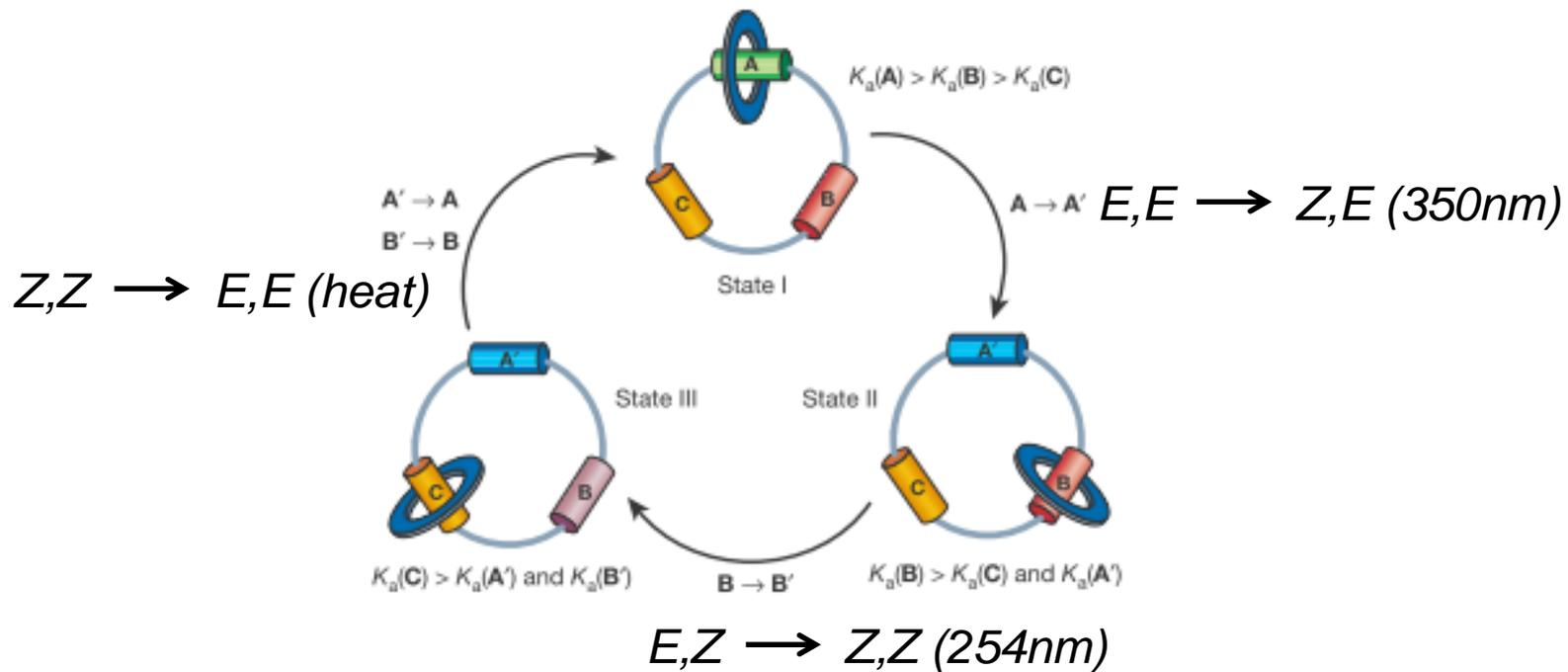


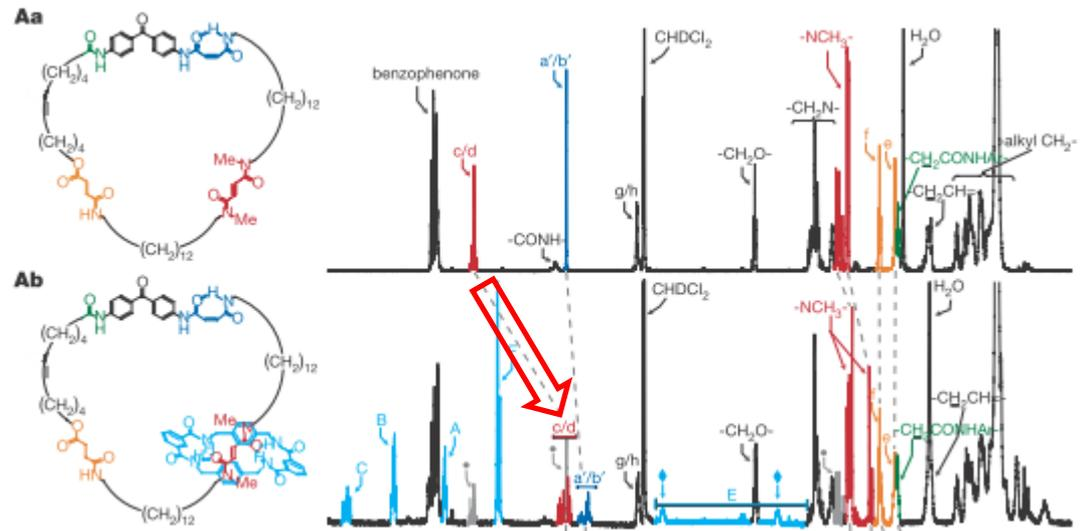
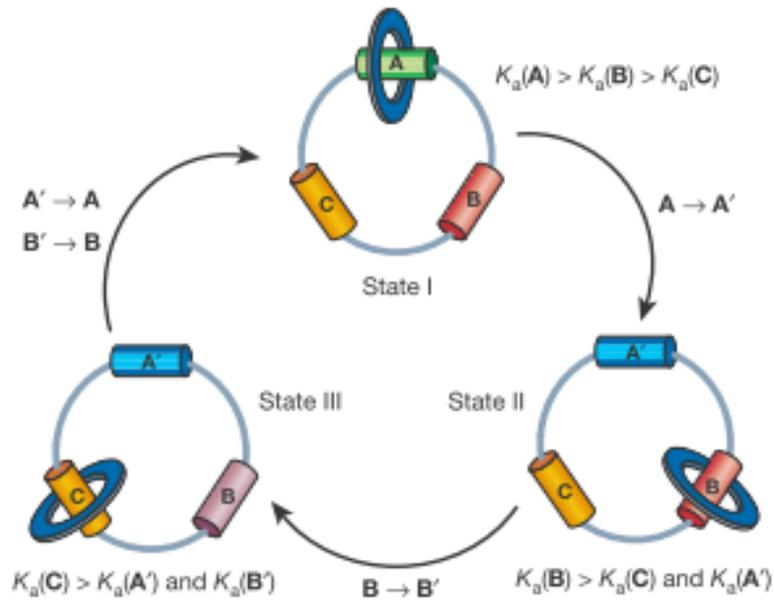
benzilamide

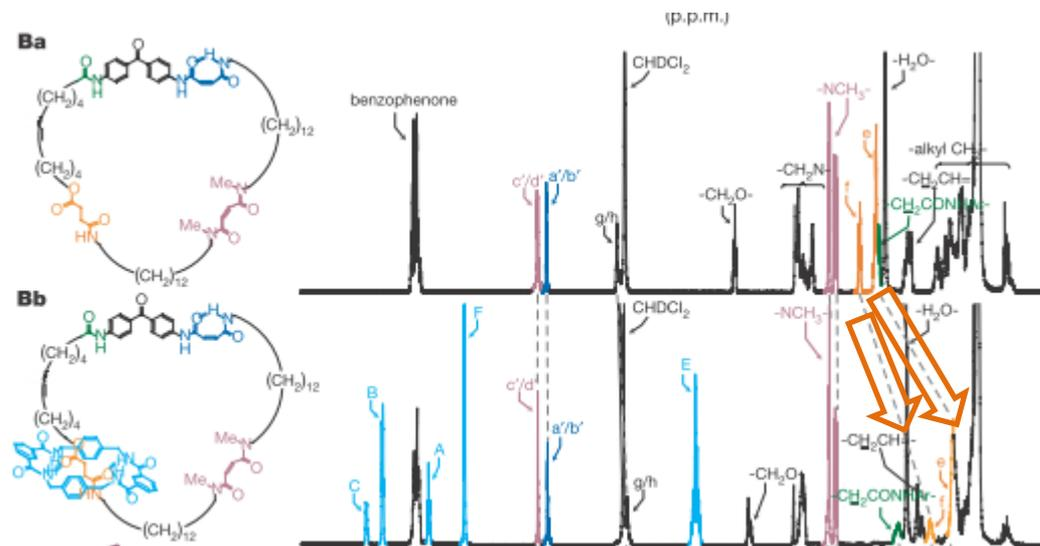
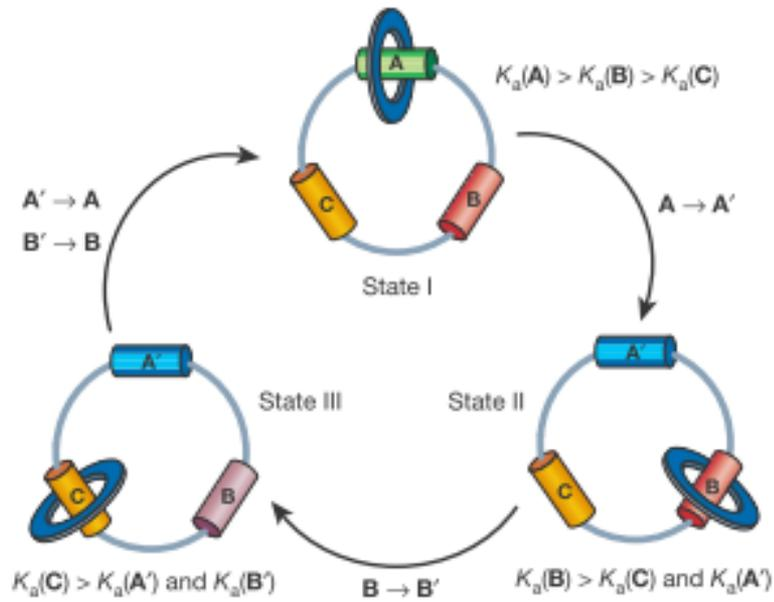


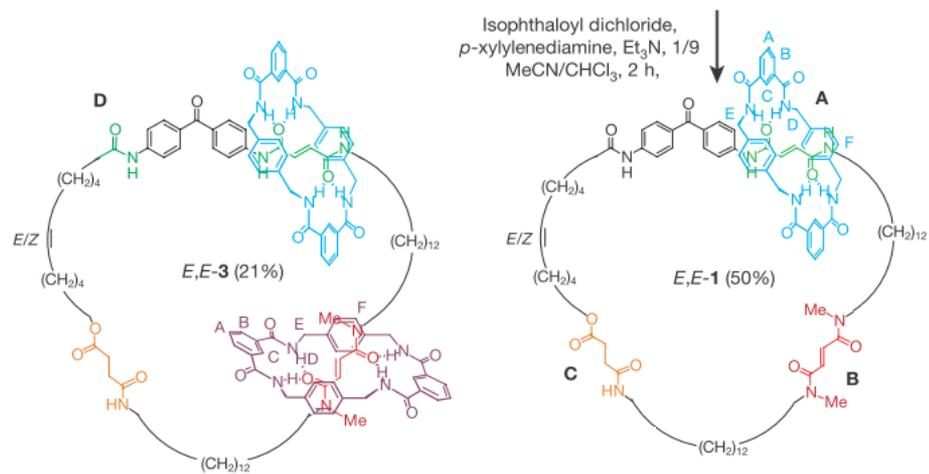
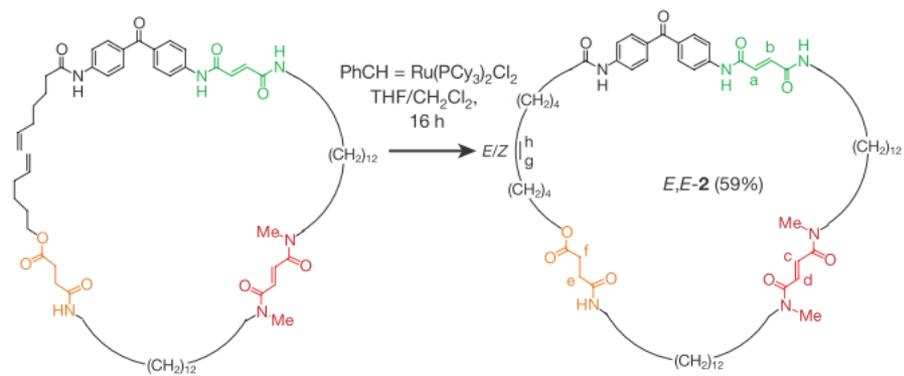
Strutture ai raggi X dei siti di binding
dei modelli [2] rotaxani con indicati
i legami idrogeno (in ordine di affinità)

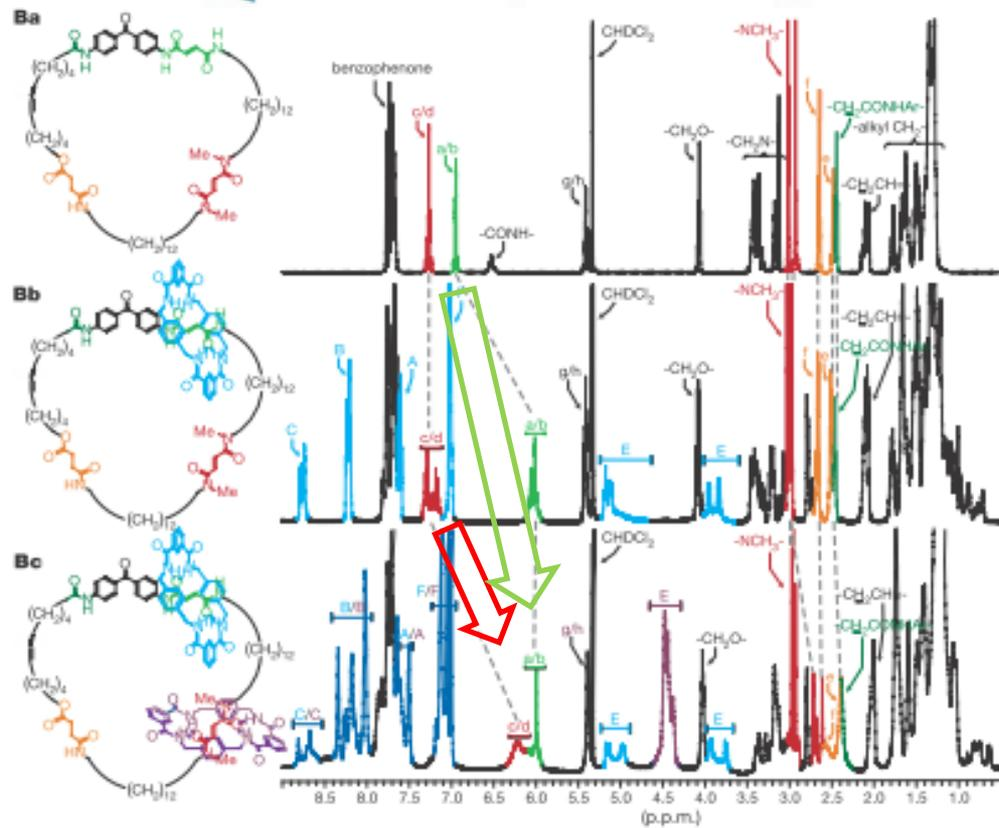












$E,E \rightarrow Z,E$ (350nm)

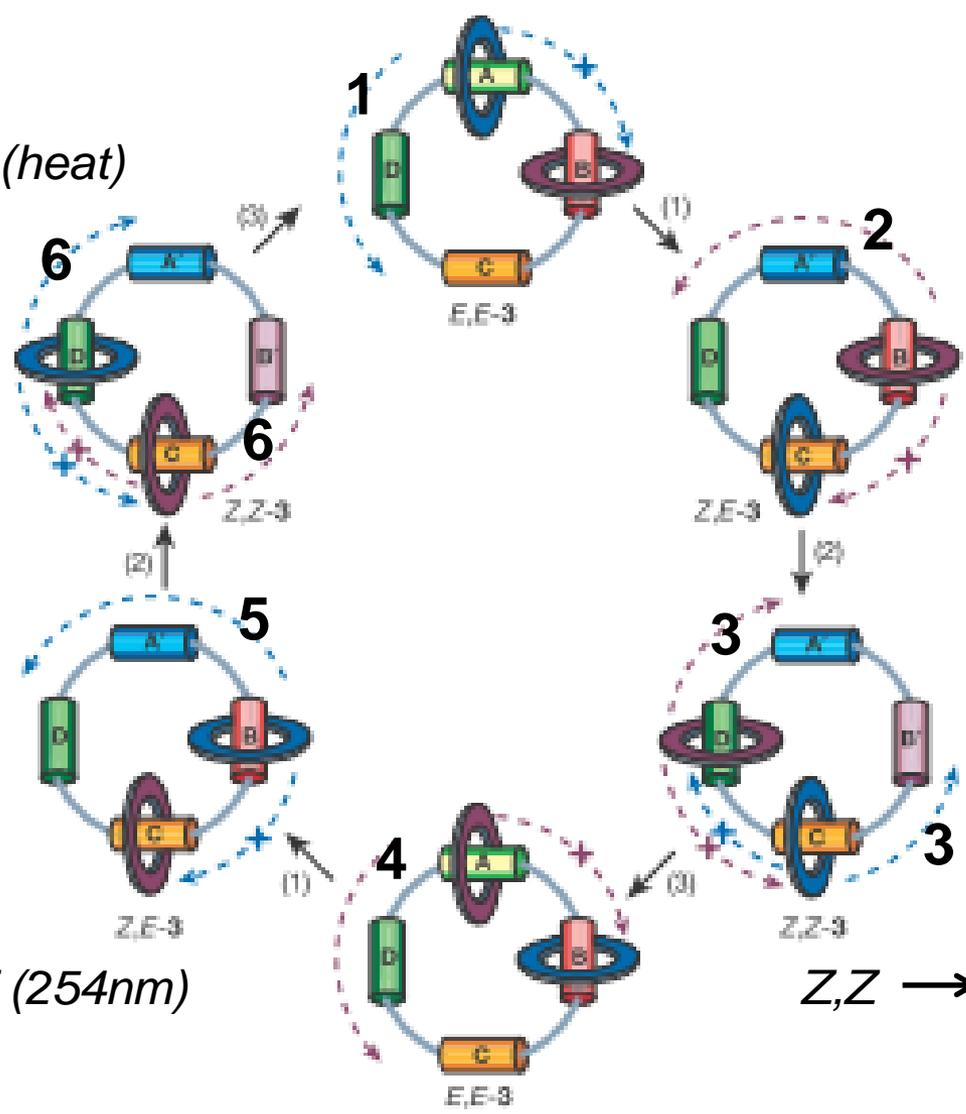
$Z,Z \rightarrow E,E$ (heat)

$E,Z \rightarrow Z,Z$ (254nm)

$E,Z \rightarrow Z,Z$ (254nm)

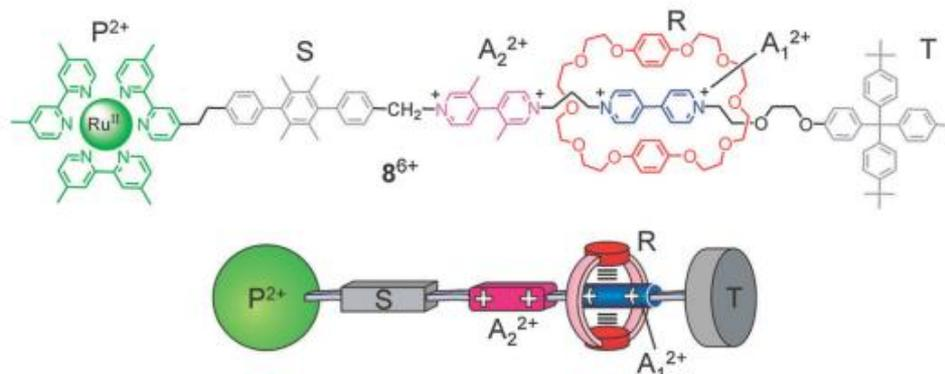
$Z,Z \rightarrow E,E$ (heat)

$E,E \rightarrow Z,E$ (350nm)

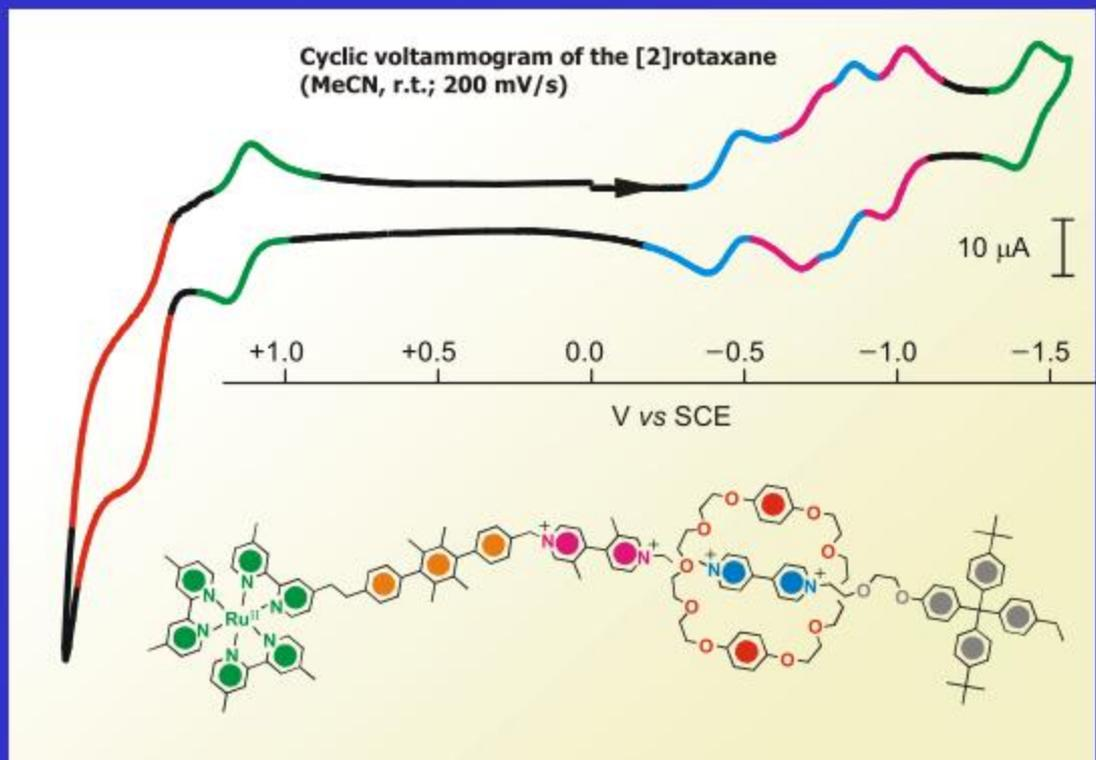
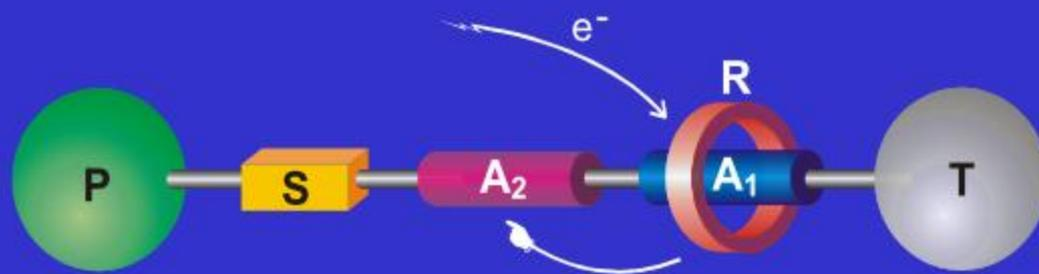


Input fotochimico

Ru(II)polypyridine complex (P^{2+})
p-terphenyl-type rigid spacer (S)
4,4'-bipyridinium (A_1^{2+})
3,3'-dimethyl-4,4'-bipyridinium (A_2^{2+})
Tetraarylmethane group (T)
Six PF_6^- counterions

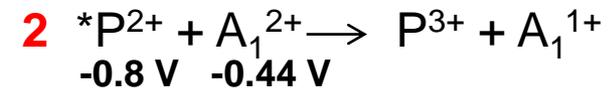
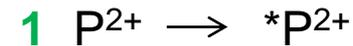
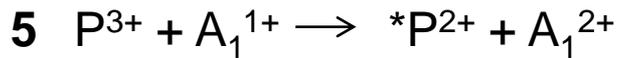
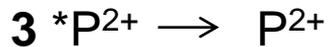
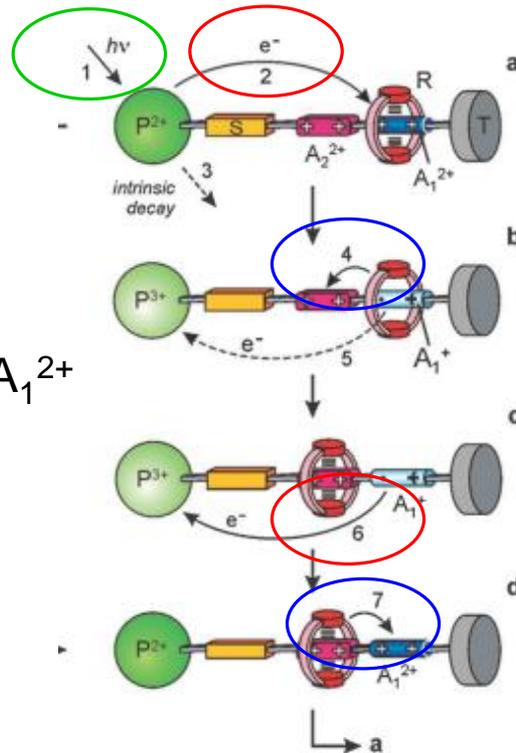
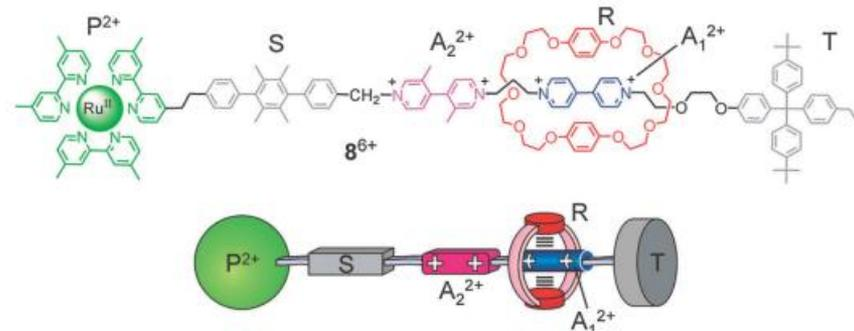


a) Redox-induced ring motion

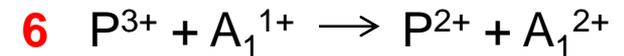


Input fotochimico

Ru(II)polypyridine complex (P^{2+})
p-terphenyl-type rigid spacer (S)
 4,4'-bipyridinium (A_1^{2+})
 3,3'-dimethyl-4,4'-bipyridinium (A_2^{2+})
 Tetraarylmethane group (T)
 Six PF_6^- counterions

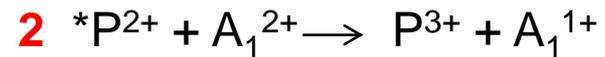
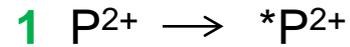
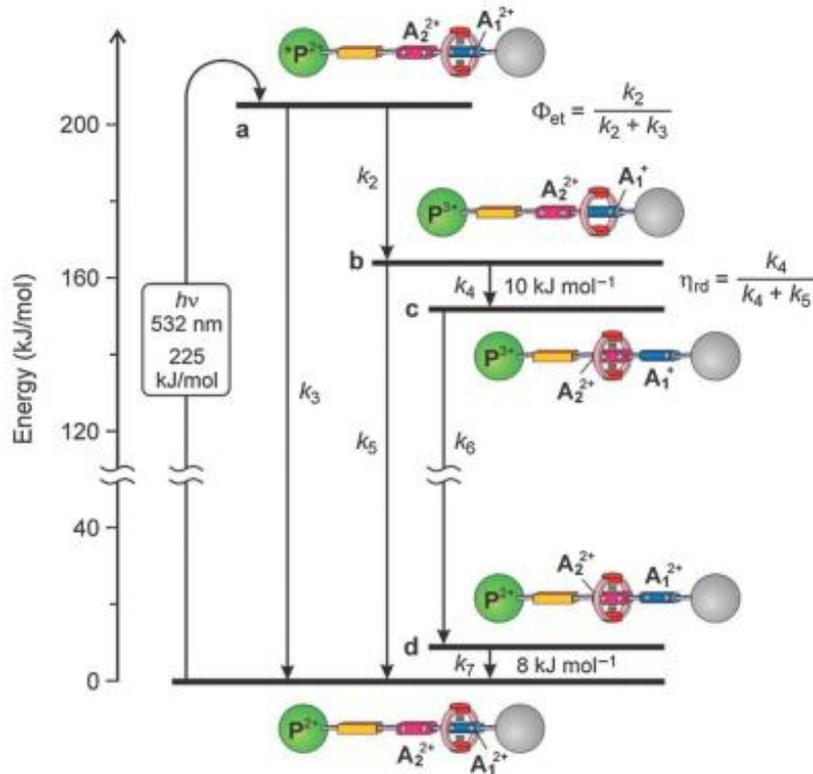


4 Shuttling (5 nm)

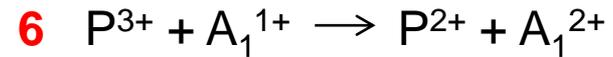


7 Shuttling (5 nm)

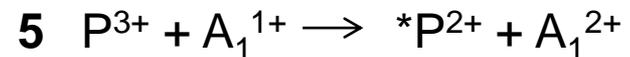
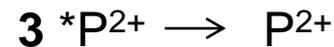
Input fotochimico



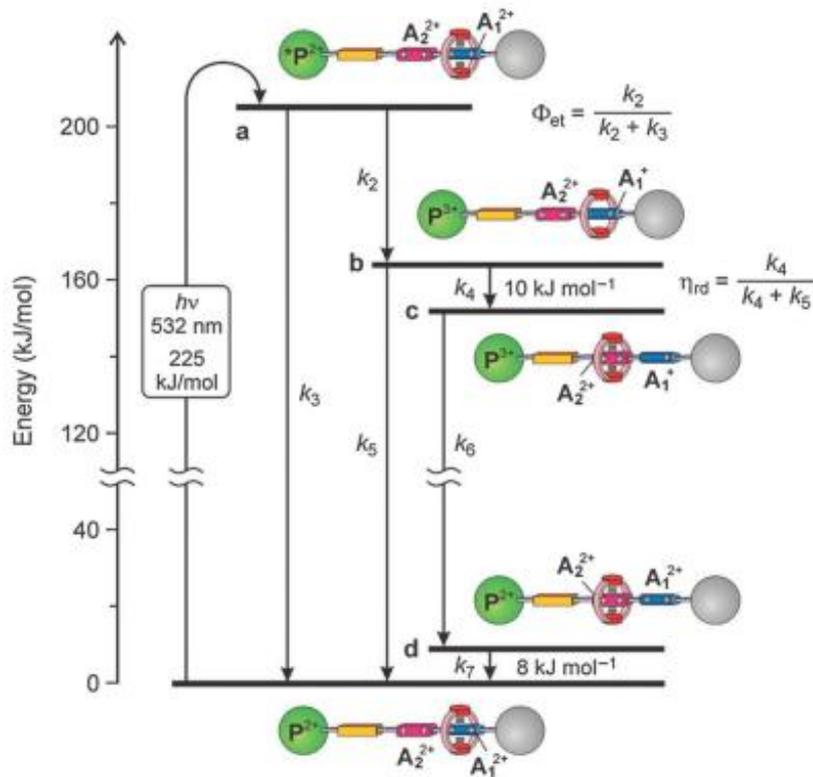
4 Shuttling (5 nm)



7 Shuttling (5 nm)



Input fotochimico



Hence, the fraction F of the excited state energy (205 kJ mol⁻¹) used for the motion of the ring amounts to *ca.* 10%, and the overall efficiency of the machine is $\eta = \Phi_{sh} \times F = 0.2\%$.

This somewhat disappointing result is compensated by the fact that the investigated system gathers together the following features: (i) it is powered by visible light (in other words, sunlight); (ii) it exhibits autonomous behaviour (*i.e.*, like natural molecular motors, it operates automatically in a constant environment as long as the energy source is available); (iii) it does not generate waste products; (iv) its operation can rely only on intramolecular processes, allowing in principle operation at the single-molecule level; (v) it can be driven at a frequency of about 1 kHz; (vi) it works in mild environmental conditions (*i.e.*, fluid solution at ambient temperature); and (vii) it is stable for at least 10³ cycles.

Input fotochimico e chimico (agenti sacrificali TEA e O₂)

